

Diverging synthesis routes and distinct properties of cubic BC₂N at high pressureZicheng Pan,¹ Hong Sun,^{1,2} and Changfeng Chen²¹*Department of Physics, Shanghai Jiao Tong University, Shanghai 200030, People's Republic of China*²*Department of Physics and High Pressure Science and Engineering Center, University of Nevada, Las Vegas, Nevada 89154, USA*

(Received 26 August 2004; published 29 November 2004)

Using first-principles total-energy and dynamic phonon calculations, we study the structural transformation to and stability of cubic BC₂N phases under pressure. We show that different starting material forms lead to distinct synthesis routes, yielding end products with drastically different physical properties. While a high-density phase with no B-B or N-N bonding shows remarkable structural stability at high pressure, a lower-density phase containing a broken covalent N-N bond displays dramatic pressure-induced collapse of bond length and a transition from a semimetal to a semiconductor, first with an indirect band gap and then a direct gap. The present work clarifies a puzzling experimental situation in BC₂N synthesis and characterization and provides a coherent picture for their interesting properties.

DOI: 10.1103/PhysRevB.70.174115

PACS number(s): 61.50.Ah, 61.50.Ks, 81.05.Zx, 71.15.Mb

The human quest for materials with superior mechanical strength or hardness has a long history that predates civilization. The crown jewel of this quest is the discovery of diamond “synthesized” in natural high-temperature and high-pressure environment deep in the Earth’s mantle. To obtain materials with properties comparable to or even exceeding those of diamond in a more controlled way, extensive efforts have been made in the last half century to synthesize strongly covalent, light-element compounds in a laboratory setting for both scientific and industrial applications, with some notable successes such as synthetic diamond and cubic boron nitride (*c*-BN). In recent years, new ternary BCN compounds have attracted considerable interest due to their outstanding performance properties, such as high melting temperature, large bulk and shear moduli, and high thermal coefficients. In particular, cubic BC₂N phases have received special attention since they are most frequently prepared in experiments and display a wide range of diverse results on structural forms and properties.^{1–3} It has been suggested⁴ that this diversity may result from the fact that these compounds belong to different metastable structures of the material. The most intriguing and controversial result is the observation that cubic BC₂N compounds prepared using different starting material forms seem to have very different structural characteristics. Knittle *et al.*¹ started from either microcrystalline BCN or a mechanical mixture of graphite and graphitic boron nitride and applied high static pressure of 30 GPa and laser heating. The resultant BC₂N has a bulk modulus of 355 GPa and a lattice constant 0.3% larger than that predicted based on an ideal mixing of diamond and *c*-BN. These results are confirmed by a more recent experiment² that employed similar synthesis conditions using ball-milled graphite and hexagonal boron nitride as the starting materials. On the other hand, Solozhenko *et al.* reported³ synthesis of cubic BC₂N from a graphitic BC₂N (*g*-BC₂N) form under high pressure (25 GPa) and laser heating. They obtained a lower-density phase with a lattice constant 1.4% larger than that of ideal mixing and a low bulk modulus (282 GPa). Previous theoretical work⁴ examined the equilibrium structures of cubic BC₂N phases at zero pressure but did not offer any insight into the pressure driven synthesis routes that can lead to

distinct cubic BC₂N phases. There is also a general lack of understanding for their structural transformations under high pressure. From fundamental and practical considerations of cubic BC₂N as a new generation of superhard materials,^{2,3} a systematic understanding of their high-pressure behavior is of crucial importance.

In this paper, we report a detailed first principles study of structural transformation toward cubic BC₂N phases from different starting material forms. We demonstrate that the use of a mixture of graphite and hexagonal boron nitride or a graphitic form of BC₂N as starting material indeed leads to distinct synthesis routes, yielding the two different cubic phases observed in the experiments. Furthermore, we present results of first principles calculations of structural and electronic properties up to 400 GPa and show that variations in local bonding characters in these two cubic BC₂N phases result in dramatic differences in their physical properties. Our results provide a comprehensive description for synthesis and characterization of cubic BC₂N at high pressure and predict remarkable stability of the high-density phase and dramatic pressure induced collapse of bond length and a semimetal to semiconductor transition in the low-density phase.

The total-energy calculations have been carried out using the local-density-approximation (LDA) pseudopotential scheme with a plane-wave basis set^{5–7} and a cutoff energy of 80 Ry. The norm-conserving Troullier-Martins pseudopotentials⁸ were used with cutoff radii of 1.3, 1.3, 1.5 a.u. for N, C, and B, respectively. The exchange-correlation functional of Ceperley and Alder⁶ as parametrized by Perdew and Zunger⁹ was used. The total energy of the structures is minimized by relaxing the structural parameters using a quasi-Newton method.¹⁰ Phonon modes of the crystal structure were calculated with the linear response theory¹¹ using the ABINIT code for the equilibrium structures obtained after the structural relaxation. This approach has been applied to systems containing B, C, and N, including layered graphitic structures, with good accuracies on structural parameters and phonon frequencies.^{4,12} In the present work, an eight-atom zinc-blende-structured unit cell is used in the calculations. Out of a total of $8!/(2!)^2 4! = 420$ different con-

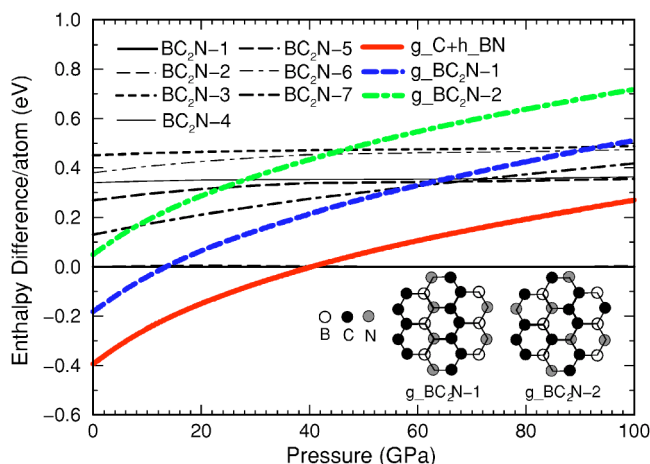


FIG. 1. (Color online) The calculated enthalpies for seven cubic BC_2N phases (see Fig. 1 of Ref. 4 for structural details) as well as three different starting material forms: a mixture of graphite and hexagonal BN (g_C+h_BN), and two forms of graphitic BC_2N (g_BC_2N-1 and g_BC_2N-2 ; the atomic arrangements in the a - b plane in the unit cells of these two structures are shown in the lower right part of the figure). The enthalpy of the most stable cubic BC_2N (BC_2N-1) is chosen as the reference and set to zero on the horizontal scale. It is practically indistinguishable from that of BC_2N-2 .

figurations only seven are topologically different, due to the high symmetry of the zinc-blende-structured lattice. These seven structures at ambient conditions have been examined in a previous work;⁴ they are taken as the starting point in the present study to explore the rich phenomena in synthesis, transformation and stability at high pressures.

Figure 1 shows the calculated enthalpies of the seven cubic BC_2N phases and three starting material forms, namely a mixture of graphite and hexagonal boron nitride, and two forms of graphitic BC_2N . The atomic arrangements in the a - b plane of the two graphitic BC_2N are shown in the figure. The g - BC_2N-1 was predicted to have the lowest energy among various *monolayer* structural models.¹³ The g - BC_2N-2 is slightly different in that a pair of the nearest-neighbor carbon and nitrogen atoms are switched in the unit cell; it is chosen because it is linked through a *continuous* deformation path with no bond breaking (therefore, low energy barrier that can be overcome by reasonable synthesis temperature) to cubic BC_2N-5 which we assign as the experimentally obtained low-density cubic phase (see below). In the present work, we have obtained the equilibrium structures of these graphitic phases by allowing full relaxation both in the a - b plane and along the c axis. We have examined both $ABAB\dots$ and $ABCABC\dots$ stacking sequences and found that the calculated enthalpies for the two stacking options are practically indistinguishable. It should be pointed out that while g_BC_2N-1 and g_BC_2N-2 with $ABCABC\dots$ stacking can deform *continuously* into the zinc-blende BC_2N-1 and BC_2N-5 , respectively, those with $ABAB\dots$ stacking will deform into the wurtzite BC_2N-1 and BC_2N-5 that are not studied here. From Fig. 1 it is seen that the two most stable cubic phases at zero pressure, BC_2N-1 and BC_2N-2 , remain nearly degenerate and most stable among

all the cubic phases under high pressure. Starting from g_C+h_BN , which corresponds to the experimental situations in the work of Knittle *et al.*¹ and Zhao *et al.*,² one would obtain BC_2N-1 or BC_2N-2 that contain no B-B or N-N bonds. These two cubic phases have been shown⁴ to have structural properties in good agreement with those reported in the abovementioned experiments. Another possible route to cubic BC_2N-1 is starting from g_BC_2N-1 with $ABCABC\dots$ stacking sequence. According to the calculated enthalpy shown in Fig. 1, the required synthesis pressure for the g_BC_2N-1 to cubic BC_2N-1 transition is actually lower. It should be emphasized that *both of these routes will not lead to the experimentally observed low-density phase of cubic BC_2N* . On the other hand, if one starts from g_BC_2N-2 , the calculated enthalpies indicate a possible transition into BC_2N-7 . However, our phonon calculations indicate that in the experimental pressure range BC_2N-7 develops imaginary phonon modes and, therefore, is unstable.¹⁴ Consequently, the enthalpy results in Fig. 1 point to a structural transformation from g_BC_2N-2 to the cubic phase BC_2N-5 around 24 GPa, in good agreement with the experiment.³

To further distinguish BC_2N-1 and BC_2N-5 and support the assignment of the latter as the experimentally obtained low-density phase, we have calculated their phonon dispersions and extracted the acoustic sound velocities. Figure 2 shows the calculated acoustic phonon bands along the $[111]$ and $[\bar{1}\bar{1}\bar{1}]$ directions in the Brillouin zone. We also performed calculations along several other directions and found that the results for BC_2N-1 are insensitive to the choice of the \mathbf{q} -vector direction, consistent with its isotropic bonding structure. However, the results for BC_2N-5 are sensitive to this choice, with values along the $[\bar{1}\bar{1}\bar{1}]$ direction significantly lower than those in the $[111]$ direction. This is caused by the orientational anisotropy of the broken covalent N-N bond in this phase.⁴ The average calculated longitudinal (V_L) and transverse (V_T) velocities are 17.14 and 10.52 km/s, respectively, for BC_2N-1 , and 14.36 and 8.33 km/s, respectively, for BC_2N-5 . The much larger values for BC_2N-1 are consistent with its higher density and elastic constants, and clearly set it apart from BC_2N-5 . The calculated sound velocities of BC_2N-5 are in good agreement with the values of $V_L=13.09\pm 0.22$ and $V_T=8.41\pm 0.14$ km/s obtained in a recent Brillouin scattering experiment¹⁵ using the same sample as in Solozhenko *et al.*'s original experiment. These dynamic phonon results that probe the overall elastic properties of the structure, combined with the previous static data on density (lattice constant) and bulk modulus,⁴ strongly support the identification of BC_2N-5 as the structure of the sample used in those experiments^{3,15} and demonstrate the crucial role played by the broken covalent N-N bond in determining its structural characteristics.¹⁶ It also suggests that g - BC_2N-2 is likely the starting graphitic BC_2N form or an intermediate structure along the synthesis route. It should be pointed out that although our \mathbf{k} -vector directional sampling is limited, our calculations (some not shown here) could not find either longitudinal or transverse sound velocities as low as those reported in the experiment¹⁵ in c - BC_2N-1 through c - BC_2N-4 . This strongly suggests that the measured results reflect the structural character of the broken N-N bonds in c - BC_2N-5 (and c - BC_2N-6 which has higher enthalpy).

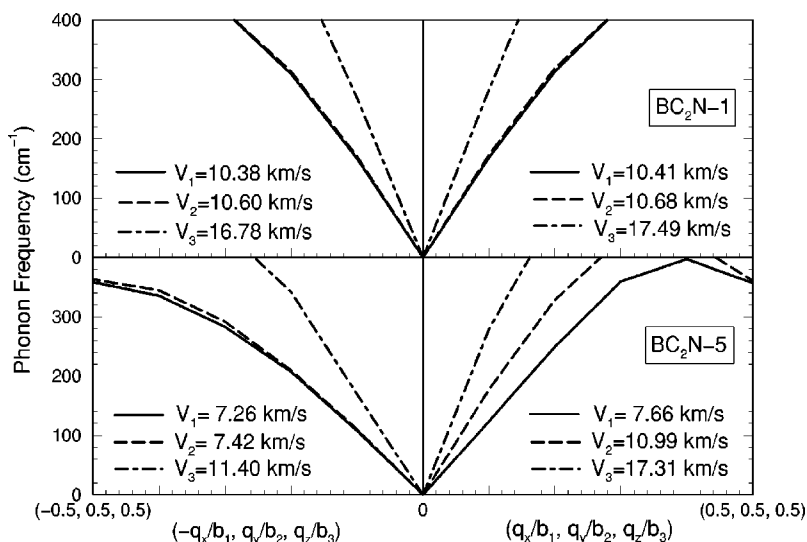


FIG. 2. The calculated phonon dispersion for BC_2N-1 and BC_2N-5 along the $[111]$ and $[\bar{1}\bar{1}\bar{1}]$ directions with the transverse (V_1 and V_2) and longitudinal (V_3) velocities indicated. The results for BC_2N-1 are nearly \mathbf{q} -independent and the two transverse branches are practically degenerate. In contrast, results for BC_2N-5 are \mathbf{q} -dependent and the two transverse branches along the $[111]$ direction split due to the orientational anisotropy of the broken N-N bond.

We now turn to a close examination of bonding and electronic properties of these BC_2N phases at high pressure. Figure 3 shows the calculated band gap and average bond lengths as a function of pressure for BC_2N-1 and BC_2N-5 . It is seen that the changes in bond lengths of BC_2N-1 are slow and smooth with increasing pressure, resulting in a gradual enhancement of the direct band gap. In contrast, the changes in bond lengths of BC_2N-5 with increasing pressure are much faster in the lower pressure range (up to 45 GPa) due to its lower density and bulk modulus with a dramatic 14% collapse in the N-N bond (with a corresponding 2% collapse in total volume) at 44–45 GPa. After this structural transformation, BC_2N-5 has a fully restored covalent N-N bond and a density close to that of BC_2N-1 . A transition from a semimetal to a semiconductor with an indirect band gap occurs at 40 GPa; the bond length collapse then induces a big jump in

the size of the gap and a transition from indirect gap to direct gap. The general trend of the band gap enhancement with increasing pressure is understood as the result of closer atomic positions and resulting stronger repulsive interactions; the transition from indirect-gap to direct-gap semiconductor in BC_2N-5 is due to the restoration of the high symmetry of the structure at high pressure and a change in the topology of the local bonding character, namely from the sp^2 bonding associated with the originally broken N-N bond to sp^3 bonding in the compressed high-symmetry structure. The LDA is known to underestimate band gap and, therefore, may lead to an overestimate of the pressure for the semimetal to semiconductor transition. A careful analysis of the band structures of BC_2N-5 indicates that the assignment of the semimetallic state is probably valid up to about 30 GPa.¹⁷ Moreover, the physical processes and mechanisms discussed

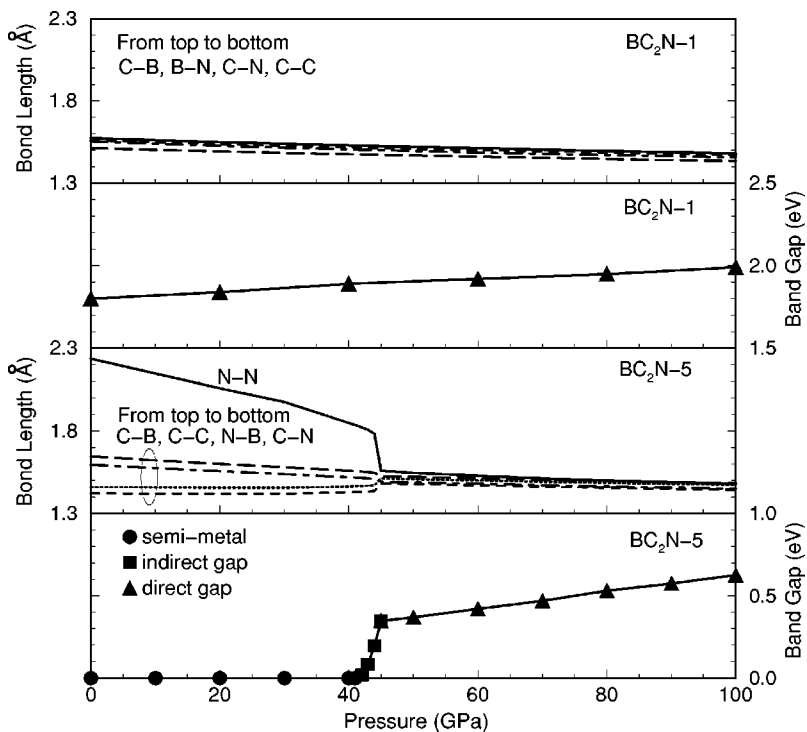


FIG. 3. The calculated band gap and average bond lengths of BC_2N-1 and BC_2N-5 as a function of pressure.

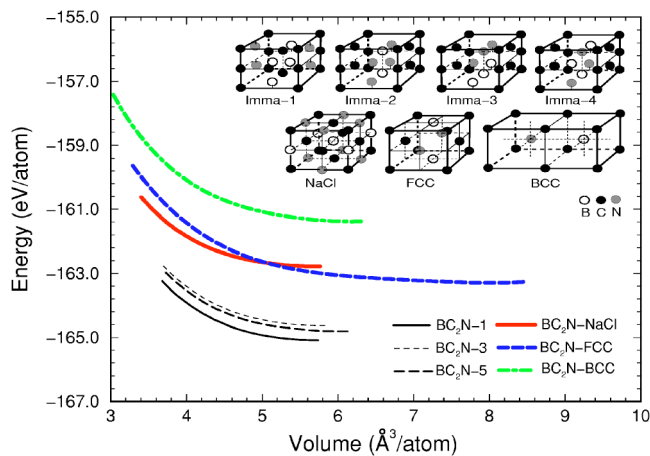


FIG. 4. (Color online) The calculated energy vs volume for three cubic BC_2N phases and the ternary analog of fcc, bcc and NaCl structures shown in the upper right part of the figure. Since the enthalpies of BC_2N -2, 4, and 6 essentially merge with those of BC_2N -1, 5, and 3, respectively, at high pressures (see Fig. 1), they are omitted for clarity. Cubic BC_2N -7 is also omitted since our phonon calculations indicate it is unstable. We also examined the four structures with Imma symmetry shown but found they are all unstable. These structures are all pressured from their equilibrium volume up to 400 GPa.

above should not be altered by any moderate quantitative correction of the transition pressure.

Finally, we examine the stability of cubic BC_2N at very high pressures and explore possible structural transformations in these ternary zinc-blende-structured covalent materials. Common candidates for high-pressure phases in corresponding binary systems include NaCl, CsCl, and binary analog of β -Sn phases.¹⁸ Here we examine ternary analog of these phases. Figure 4 shows the calculated energy versus volume results for cubic BC_2N phases of interest, together with those for ternary analog of face-centered-cubic (fcc), body-centered-cubic (bcc), and NaCl structures of BC_2N . It is seen that both BC_2N -1 and BC_2N -5 are stable up to the highest pressure calculated (400 GPa), with no sign of a

phase transition to each other or to other phases. We also have conducted a careful search for stable BC_2N phases with Imma symmetry. The structures of four possible Imma phases are shown in Fig. 4. Our calculations did not find any stable BC_2N structure with Imma symmetry. This extends to a ternary system the previous conclusions for binary zinc-blende-structured systems where extensive search for Imma phases did not yield any stable structures.¹⁹

In summary, our first-principles total-energy and dynamic phonon calculations reveal that different starting material forms lead to diverging synthesis routes and distinct physical properties for cubic BC_2N . This may be a general phenomenon in the synthesis of covalently bonded materials with complex compositional and structural characters. The present calculations confirm and explain the experimentally observed variation in structural forms of synthesized cubic BC_2N . It is predicted that the high-density BC_2N phase will exhibit superb stability to very high pressure and the low-density phase will display a dramatic pressure-induced bond-length (volume) collapse around 44–45 GPa and a concomitant transition from a semimetal to a semiconductor, with an initial indirect band gap turned into a direct band gap coinciding with the bond length/volume collapse. These results establish a comprehensive understanding for the synthesis routes, structural transformation and stability, and interesting physical properties of cubic BC_2N at high pressure. The present work shows that first-principles calculations can be used, in close collaboration with experiments, to clarify how various metastable structures with distinct properties might be synthesized. This approach may be pursued effectively in the study of novel materials in the future.

We thank Yusheng Zhao for discussions on experiments. H.S. acknowledges useful discussions on BC_2N at ambient conditions with Marvin L. Cohen and Steven G. Louie. This work was supported in part by the DOE under Cooperative Agreement No. DE-FC52-01NV14049 at UNLV. H.S. was also supported by the NNSF of China under Grant No. 10274050 and computing resources at the High Performance Computing Center at Shanghai Jiao Tong University.

¹E. Knittle, R. B. Kaner, R. Jeanloz, and M. L. Cohen, *Phys. Rev. B* **51**, 12149 (1995).
²Y. S. Zhao, D. W. He, L. L. Maemen, D. T. Shen, R. B. Schwarz, Y. Zhu, D. L. Bish, J. Huang, J. Zhang, G. Shen, J. Qian, and T. W. Zerda, *J. Mater. Res.* **17**, 3139 (2002).
³V. L. Solozhenko, D. Andrault, G. Fiquet, M. Mezouar, and D. C. Rubie, *Appl. Phys. Lett.* **78**, 1385 (2001).
⁴H. Sun, S. H. Jhi, D. Roundy, M. L. Cohen, and S. G. Louie, *Phys. Rev. B* **64**, 094108 (2001).
⁵J. Ihm, A. Zunger, and M. L. Cohen, *J. Phys. C* **12**, 4409 (1979).
⁶D. M. Ceperley and B. J. Alder, *Phys. Rev. Lett.* **45**, 566 (1980).
⁷M. L. Cohen, *Phys. Scr.*, T **11**, 5 (1982).
⁸N. Troullier and J. L. Martins, *Phys. Rev. B* **43**, 1993 (1991).
⁹J. P. Perdew and A. Zunger, *Phys. Rev. B* **23**, 5048 (1981).
¹⁰B. G. Pfommer, M. Cote, S. G. Louie, and M. L. Cohen, *J.*

Comput. Phys. **131**, 233 (1997).

¹¹X. Gonze, *Phys. Rev. B* **55**, 10337 (1997); X. Gonze and C. Lee, *ibid.* **55**, 10355 (1997).

¹²H. Sun, F. J. Ribeiro, J. L. Li, D. Roundy, M. L. Cohen, and S. G. Louie, *Phys. Rev. B* **69**, 024110 (2004).

¹³A. Y. Liu, R. M. Wentzcovitch, and M. L. Cohen, *Phys. Rev. B* **39**, 1760 (1989).

¹⁴This example shows that dynamic phonon instability could fundamentally alter the synthesis routes and phase diagram. As a result, phonon calculations should be combined with the usual energy/enthalpy criteria in determining the structural stability.

¹⁵S. N. Tkachev, V. L. Solozhenko, P. V. Zinin, M. H. Manghani, and L. C. Ming, *Phys. Rev. B* **68**, 052104 (2003).

¹⁶Using larger unit cells in the calculation will introduce more structural configurations. However, judging from the excellent

agreement between our results and experimental data, it is unlikely to change the underlying physics dictated by the broken N-N bond configuration that has already been captured by the 8 atom unit cell.

¹⁷The calculated electronic bands of BC₂N-5 up to 30 GPa show conduction and valence band crossings at the same k points at the Fermi level, a situation reminiscent of that in semimetallic graphite [J. C. Boettger, Phys. Rev. B **55**, 11202 (1997)]. Meanwhile, starting at 40 GPa, the conduction band minimum and

valence band maximum shift apart significantly, which may allow a band gap to open in more accurate calculations such as the GW scheme [A. Fleszar, Phys. Rev. B **64**, 245204 (2001)]. A systematic examination of the pressure driven evolution of the band structures of BC₂N-5 will be presented elsewhere.

¹⁸A. Mujica, A. Rubio, A. Munoz, and R. J. Needs, Rev. Mod. Phys. **75**, 863 (2003).

¹⁹R. J. Nelmes, M. I. McMahon, and S. A. Belmonte, Phys. Rev. Lett. **79**, 3668 (1997).